Probabilistic Analysis of Soil-Structure Interaction in a Single-Span Railway Bridge Using the Error-Domain Model Falsification Method

Seyed Amin Hosseini Tehrani[1][0009-0008-5895-8103], Imane Bayane[1][0000-0002-0928-9790], Andreas Andersson[1,2][0000-0002-8926-2140], Abbas Zangeneh Kamali[1,3][0000-0001-6875-2477], and Jean-marc Battini[1][0000-0003-2104-382X]

[1] KTH Royal Institute of Technology, Stockholm, Sweden
[2] Swedish Transport Administration, Solna, Sweden
[3] ELU Konsult AB, Stockholm, Sweden

Abstract. In this paper, the performance of a single-span railway bridge with integrated retaining walls during high-speed train passage is investigated by considering different uncertainties originating from modeling assumptions and measurement processes. For this purpose, a single-span railway bridge is equipped with numerous accelerometers and is excited using a hydraulic actuator across different frequency ranges. A comprehensive 3D model of the bridge and the surrounding soils is created in Abaqus. Different sets of material properties for concrete and soil components are derived by converging the frequencies and damping ratios of the first three structural modes, using both the Error-Domain Model Falsification (EDMF) and Residual Minimization (RM) methods. These material properties are subsequently utilized in high-speed train passage analysis, and the results are compared.

Keywords: Resonance of railway bridges · Soil–structure interaction · Error-domain model falsification.

1 Introduction

The train-induced loading is periodic in nature, with the excitation frequency being dependent on the axle distance of the train and its velocity [1, 2]. High-speed trains exhibit a broader excitation frequency range compared to conventional commuter trains due to their increased speed. The excitation frequency of a high-speed passing train may align with the natural frequencies or subharmonics of a bridge, potentially causing resonance [3]. Resonance in bridges can lead to structural damage, posing risks to passengers and increasing maintenance costs. Consequently, design standards have established vibration limits for railway bridges during high-speed train passage. For instance, Eurocode limits the maximum acceleration response of a railway bridge to 3.5 m/s^2 for ballasted tracks and 5 m/s^2 for ballastless tracks [4]. Accurate analysis and prediction of resonance responses are thus crucial. The resonance response of a railway bridge is influenced by its modal properties, particularly the first bending mode [5, 6]. Moreover, the modal properties of buried structures, such as railway bridges with integrated retaining walls, are influenced significantly by surrounding soils, necessitating the inclusion of Soil-Structure Interaction (SSI) effects in the dynamic analyses of the railway bridge [7, 8].

Error-Domain Model Falsification (EDMF) is a data-interpretation methodology that is based on the idea that data should not be used to validate models (considered weak science) but rather to falsify them (considered strong science) [9, 10]. It has been implemented for a range of structural identification purposes, including fatigue-life assessment [11–13], damage evaluation [14, 15], and ultimate limit state verification [16, 17]. In civil engineering, conservative and simplified models are typically employed to design structures. These models include notable uncertainties resulting from approximations and assumptions.

Within the EDMF framework, any model instance that yields predictions incompatible with observed measurements is falsified. Compatibility thresholds are established by considering uncertainties stemming from modeling assumptions and measurement processes. The quantification of these uncertainties for full-scale applications frequently requires specialized engineering expertise.

Residual Minimization (RM) is another method that is widely used in practice due to its computational efficiency; however, measurement and model uncertainties, as well as biases, are not considered. In contrast, EDMF has been successfully applied to more than 20 full-scale data-interpretation challenges [12, 18] and has been shown to provide more accurate structural identification than RM and traditional Bayesian model updating. Comparisons of these methodologies have been conducted on numerous full-scale case studies [11, 12] as well as on theoretical examples where the ground truth is known.

In this study, the effect of SSI on the dynamic response of a single-span end-shield bridge during high-speed train passage is analyzed. For this purpose, the bridge is equipped with multiple accelerometers and is excited by a hydraulic actuator at various frequencies and load amplitudes. A complete three-dimensional numerical model of the bridge-soil system is created in Abaqus/Cae (v6.24) and updated against the experimental data. Two model updating methods, EDMF and RM, are employed, and the corresponding acceleration responses of the bridge during high-speed train passage are compared.

2 Methodology

2.1 Error-Domain Model Falsification

In this method, feasible ranges of essential parameters are first identified, and an Initial Model set (IMS) is established by sampling from these ranges. Measurements and associated uncertainty information are subsequently applied to falsify models within the IMS, resulting in a Candidate Model Set (CMS) that properly explains the observed behavior. Several model classes may be potential candidates for describing the behavior of a system. These model classes take system properties as arguments, including geometry, material properties, boundary conditions, and loading.

The true response of the system, Q, is approximated by model predictions $g_k(\theta_k)$ for a set of parameters θ_k, where $\epsilon_{\text{model},k}$ represents the modeling error. Similarly, the true response is captured by measurements y, accompanied by measurement error $\epsilon_{\text{measure}}$. This relationship is expressed by the following equation.

$$g_k(\theta_k) + \epsilon_{\text{model},k} = Q = y + \epsilon_{\text{measure}}$$

Modeling uncertainties are introduced by factors such as material properties, geometrical properties, mesh refinement, boundary conditions, connections, and other simplifications in the model. These uncertainties are estimated through engineering judgment. Measurement uncertainties arise from variables including sensor resolution, position, load, field conditions, and human error. Estimations of these uncertainties are based on specifications provided by the sensor manufacturer and through repeated testing. Uncertainties originating from both modeling and measurement are combined to estimate the combined uncertainty, U_c.

The combined uncertainty, U_c, is utilized to set criteria for model falsification. Thresholds are established based on a target reliability of 95% ($\Phi = 0.95$), which is typically required for civil engineering applications. These thresholds are calculated to ensure that the model reliably identifies true system behavior within this confidence interval.

For each measurement, the lower and upper bounds of the thresholds, T_{low} and T_{high}, are determined. These bounds are derived such that the integral of the probabilistic distribution function f_{U_c} from T_{low} to T_{high} correlates to the target reliability (Φ).

Falsification occurs when a model prediction of any measurement scenario is found incompatible with these defined thresholds. This incompatibility is assessed using the equation:

$$g_k(\theta_k) - y \notin [T_{\text{low}}, T_{\text{high}}]$$

Model instances that are not falsified are grouped into the CMS. In these instances, structural behavior remains consistent with observed data, and uncertainties arising from both modeling and measurement are taken into consideration.

2.2 Residual Minimization

The Residual Minimization (RM) method, known for its computational efficiency, operates under the assumption that the discrepancies between model predictions and actual measurements are attributed to zero-mean uncertainty distributions. This method is updated by optimizing model parameter values that reduce the error between simulation results and observational data. The optimization is governed by the following objective function:

$$\hat{\theta} = \arg\min_{\theta} \sum_{i=1}^{n_y} \left(\frac{g_i(\theta) - y_i}{y_i} \right)^2$$

Here, $g_i(\theta)$ represents the model response corresponding to the parameter set θ, while y_i denotes the measured value at each measurement point. The total number of measurement points is given by n_y. The parameter set $\hat{\theta}$ is obtained by minimizing the squared normalized residuals across all data points.

3 Experimental testing

The Aspan bridge [19–21], shown in Figure 1, is a reinforced, continuous, single-span concrete slab railway bridge located on the Bothnia line north of Sweden. It features a span length of 24 m. The bridge deck extends beyond the end supports and is embedded in the backfill soil through the wing walls and retaining walls, which are referred to as the "end shields." The lengths of the cantilever sections are 1.7 m. The end supports are made of two walls placed on shallow foundations.

Fig. 1: Side view of the single-span railway bridge and the hydraulic actuator.

Figure 2 illustrates the layout of sensor placement and the positioning of the hydraulic actuator on the bridge. Throughout the forced vibration experiments, the hydraulic actuator was positioned beneath the edge beam, approximately 2.9 m from the left end support, resulting in the excitation of both bending and torsional modes. The experiments were performed at varying load amplitudes with a low-frequency sweep rate to ensure the accurate calculation of Frequency Response Functions (FRFs) at each accelerometer. The FRF vector (H) at each sensor was obtained by dividing the measured acceleration signal in the frequency domain by the input force. The results from the 5 kN test were utilized in this study. The FRF at sensor A3 is shown in Figure 3. The Half-Power Bandwidth method (HPB) was applied to determine the modal properties of the first three structural modes. The identified modal properties, including the natural frequencies and modal damping ratios of the first two bending modes and the first torsional mode are presented in Table 1.

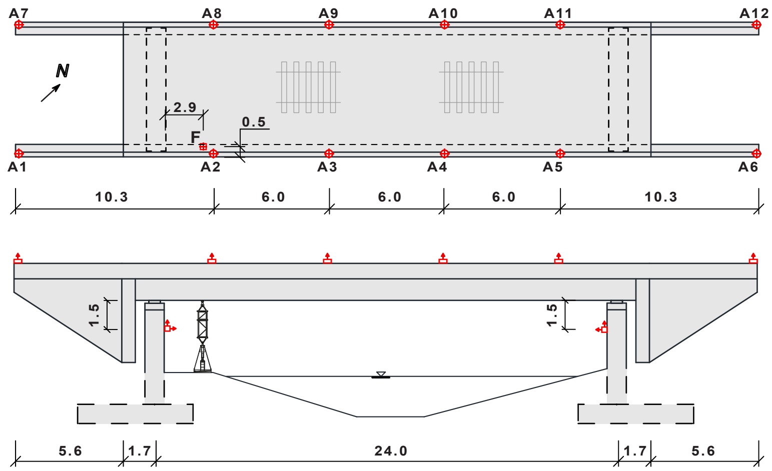

Fig. 2: Plan drawing and sensor placement of the single-span railway bridge.

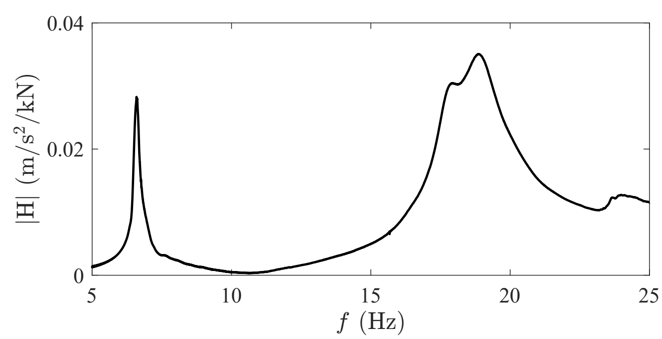

Fig. 3: FRF at sensor A3 for the 5 kN test.

4 Numerical model

The 3D model utilized for the railway bridge-soil system is illustrated in Figure 4 [19]. This model features two types of soil: the backfill soil, in contact with the end shields, and the underpinning soil, positioned directly beneath the

Table 1: Modal properties of the forced vibration experiment using the HPB method.

$\mathbf{F_{amp}}$ **(kN)**	**First bending**		**Second bending**		**First torsion**	
	f_1 (Hz)	ξ_1 (%)	f_2 (Hz)	ξ_2 (%)	f_3 (Hz)	ξ_3 (%)
5	6.6	1.2	17.8	2.5	18.8	3.7

foundations. The backfill soil elements are longitudinally extended by 20 meters from the wing walls to ensure a sufficient medium for bridge-soil interaction. The soil dimensions were determined based on a convergence study, ensuring that further increases would not significantly alter the dynamic response of the system. Infinite elements were applied at the boundaries of the backfill soil to mitigate wave reflection effects.

In the Finite Element (FE) model, the concrete bridge, footings, underpinning soil, ballast, and sleepers were discretized using 20-noded quadratic solid elements (C3D20). The backfill soil was modeled by 10-noded quadratic tetrahedral solid elements (C3D10). Based on a convergence study, a mesh size of 0.6 m was adopted for the bridge, footings, and ballast, while 1.5 m was selected for the soil components, ensuring at least nine nodes per wavelength at 30 Hz [22]. The rails, characterized by UIC60 beam sections, were modeled using shear-flexible 2-node linear beam elements (B31) and were connected to the sleepers via horizontal and vertical springs. The stiffness of these springs was adjusted to meet Eurocode standards, with values set at 150 MN/m vertically and 2.5 MN/m horizontally. The surrounding soils and ballast, assumed to be within low shear strain levels, are modeled as linear elastic materials.

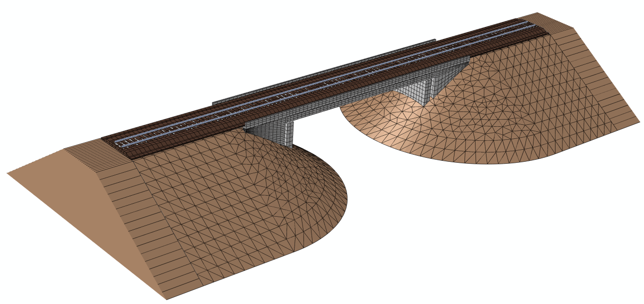

Fig. 4: 3D model of the Aspan bridge and the surrounding soils in Abaqus.

In this study, three material properties were considered for the model updating of the bridge: the elastic modulus of the concrete (E_c), underpinning soil (E_{s1}), and backfill soil (E_{s2}). These properties were selected due to their significant impact on the dynamic behavior of the bridge-soil system, especially for higher modes. The elastic modulus values considered for the concrete ranged from 38 GPa to 43 GPa in increments of 1 GPa. For both the backfill and underpinning soils, the elastic modulus varied from 100 MPa to 500 MPa in steps of 100 MPa. A total of 150 datasets of these material properties were utilized to structurally identify the model to the experimental data using both EDMF and RM methods. The initial phase of model updating involved the comparison of natural frequencies across three structural modes. Ultimately, both natural frequencies and damping ratios were utilized for comprehensive model validation.

5 Results

In Table 2, the uncertainties associated with the model, sensor inaccuracies, repeatability, and actuator variability are presented. It is assumed that these uncertainties follow a uniform distribution within the specified ranges. The first candidate model set is obtained by considering these uncertainties and comparing the natural frequencies between the measurements and the numerical model, which yields 25 sets of parameters. When both the natural frequencies and damping ratios are compared, 5 parameter sets are obtained. In Figure 5a, all 150 sets of parameters are depicted with gray lines, while the sets obtained using the EDMF method for frequency comparisons (EDMF_f) are shown in blue lines, and those for both frequency and damping ratio comparisons ($\mathrm{EDMF}_{f\&d}$) are in red lines.

The results from the RM method are presented in Figure 5b. It is observed that the RM method yields a single solution when comparing natural frequencies (RM_f) and a single solution when comparing both frequencies and damping ratios ($\mathrm{RM}_{f\&d}$), with both solutions minimizing the residuals between the measured and simulated results. These solutions are included in the set obtained by the EDMF method, and it is evident that they do not reflect all possible outcomes derived from the considered uncertainties.

Table 2: Uncertainty sources and their distributions.

Source	**Min**	**Max**	**Distribution**
Model	−10%	5%	Uniform
Sensor	−0.01%	0.01%	Uniform
Load	−0.01%	0.01%	Uniform
Repeatability	−0.05%	0.05%	Uniform

High-speed train passage analysis was conducted using the 3D model of the bridge-soil system with five material sets obtained from $\mathrm{EDMF}_{f\&d}$ method and the parameter set derived from the $\mathrm{RM}_{f\&d}$ method. The model was subjected to the design train load model (HSLM-A9) as specified by Eurocode for train

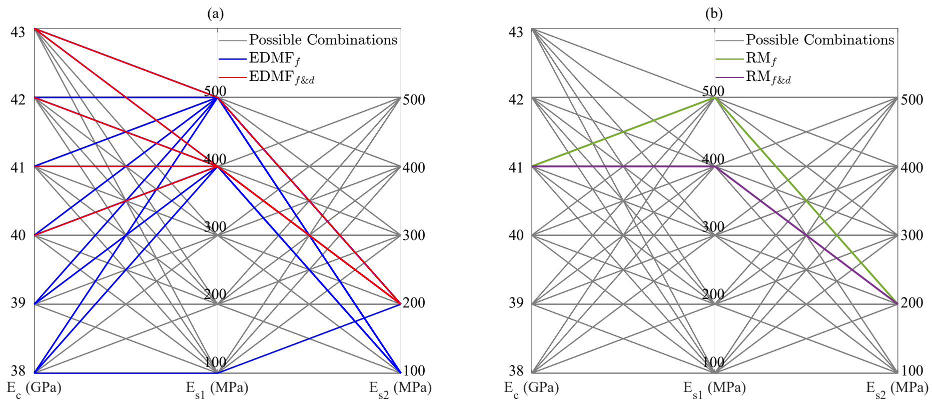

Fig. 5: Possible outcomes using EDMF and RM methods.

speed ranging from 150 to 350 km/h. This specific load model was selected because it creates the highest acceleration response in the bridge. The analysis was performed in the frequency domain by applying moving point loads on the rail elements and calculating the transfer functions between the excitation point on the rails and the response point at the center of the bridge deck. Modal superposition, incorporating all mode shapes up to 20 Hz, was employed. The resulting data are displayed in Figure 6. The train passage results using the EDMF set of parameters are illustrated with upper and lower bounds in acceleration amplitude. Notably, the peak response around 310 km/h corresponds to the second subharmonic of the first bending mode. Various uncertainties are included in the EDMF method, resulting in a range for the acceleration response of the bridge. In contrast, the results from the RM method represent just one of the possible solutions. When uncertainties were taken into account, minor variations in the high-speed train passage response were identified. However, these discrepancies were not critical for this particular bridge since the response remained well below the Eurocode limit of 3.5 m/s^2. In cases where bridge response approaches this limit, incorporating uncertainties and evaluating all different sets of parameters becomes essential.

6 Conclusions

In this paper, a single-span end-shield bridge is studied both numerically and experimentally. For this purpose, the bridge was equipped with numerous accelerometers and excited at various frequencies and load amplitudes using a hydraulic actuator. FRFs were obtained at each sensor location, and the HPB method was used to identify the natural frequencies and damping ratios of the first two bending modes and the first torsional mode of the bridge. A full 3D model of the bridge and surrounding soils was then created in Abaqus and updated to the experimental data using the EDMF and RM methods.

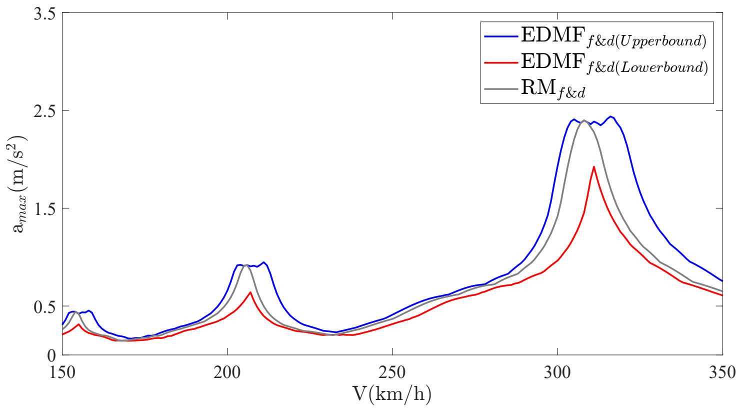

Fig. 6: Comparison of HSLM-A9 train passage results using material properties derived from $EDMF_{f\&d}$ (upper and lower bounds) and $RM_{f\&d}$.

In total, 150 initial model sets were generated by changing the elastic modulus of the concrete and surrounding soils. When only the natural frequencies of the three structural modes were compared using EDMF, 25 data sets were identified as candidate models. When both natural frequencies and damping ratios were compared, 5 data sets were obtained. In contrast, the RM method produced a single solution in both cases.

Ultimately, the train passage results using these different sets of parameters were presented and compared. By including various uncertainties related to modeling and measurement, a range for the acceleration response of the bridge is obtained, highlighting that results from RM are just one of the possible solutions. This is particularly critical for bridges where the acceleration response is close to the 3.5 m/s^2 limit, as discrepancies can lead to different conclusions. As a result, including uncertainties in the dynamic analysis of end shield bridges for high-speed train passage is crucial, and EDMF can be a suitable alternative for this purpose.

References

1. C. E. Inglis, A mathematical treatise on vibrations in railway bridges, Cambridge University Press, 2015.
2. L. Frỳba, Vibration of solids and structures under moving loads, Vol. 1, Springer science & business media, 2013.
3. H. Xia, N. Zhang, W. Guo, Analysis of resonance mechanism and conditions of train–bridge system, Journal of Sound and Vibration 297 (3-5) (2006) 810–822.
4. Eurocode 1: Actions on structures–part 2: Traffic loads on bridges (2003).
5. A. Zangeneh, C. Svedholm, A. Andersson, C. Pacoste, R. Karoumi, Dynamic stiffness identification of portal frame bridge–soil system using controlled dynamic testing, Procedia engineering 199 (2017) 1062–1067.

6. S. A. H. Tehrani, A. Andersson, A. Zanganeh, J.-M. Battini, Dynamic soil–structure interaction of a three-span railway bridge subject to high-speed train passage, Engineering Structures 301 (2024) 117296.
7. A. Zangeneh, S. François, G. Lombaert, C. Pacoste, Modal analysis of coupled soil-structure systems, Soil Dynamics and Earthquake Engineering 144 (2021) 106645.
8. S. A. Hosseini Tehrani, A. Zangeneh, A. Andersson, J.-M. Battini, Dynamic soil-structure interaction of a continuous railway bridge, in: XII International Conference on Structural Dynamics (Eurodyn 2023), Delft, The Netherlands, 02-05 July 2023, 2023.
9. K. Popper, The logic of scientific discovery, Routledge, 2005.
10. J.-A. Goulet, I. F. Smith, Structural identification with systematic errors and unknown uncertainty dependencies, Computers & structures 128 (2013) 251–258.
11. S. G. Pai, A. Nussbaumer, I. F. Smith, Comparing structural identification methodologies for fatigue life prediction of a highway bridge, Frontiers in Built Environment 3 (2018) 73.
12. R. Pasquier, J.-A. Goulet, C. Acevedo, I. F. Smith, Improving fatigue evaluations of structures using in-service behavior measurement data, Journal of Bridge Engineering 19 (11) (2014) 04014045.
13. R. Pasquier, L. D'Angelo, J.-A. Goulet, C. Acevedo, A. Nussbaumer, I. F. Smith, Measurement, data interpretation, and uncertainty propagation for fatigue assessments of structures, Journal of Bridge Engineering 21 (5) (2016) 04015087.
14. Y. Reuland, P. Lestuzzi, I. F. Smith, Measurement-based support for post-earthquake assessment of buildings, Structure and Infrastructure Engineering 15 (5) (2019) 647–662.
15. Y. Reuland, P. Lestuzzi, I. F. Smith, A model-based data-interpretation framework for post-earthquake building assessment with scarce measurement data, Soil Dynamics and Earthquake Engineering 116 (2019) 253–263.
16. M. Proverbio, D. G. Vernay, I. F. Smith, Population-based structural identification for reserve-capacity assessment of existing bridges, Journal of civil structural health monitoring 8 (3) (2018) 363–382.
17. D. G. Vernay, F.-X. Favre, I. F. Smith, Robust model updating methodology for estimating worst-case load capacity of existing bridges, Journal of Civil Structural Health Monitoring 8 (5) (2018) 773–790.
18. I. F. Smith, Studies of sensor data interpretation for asset management of the built environment, Frontiers in Built Environment 2 (2016) 8.
19. S. A. H. Tehrani, A. Zanganeh, A. Andersson, J.-M. Battini, Simplified soil–structure interaction modeling techniques for the dynamic assessment of end shield bridges, Engineering Structures 319 (2024) 118803.
20. A. Albright, J.-M. Battini, A. Andersson, Dynamic soil-structure interaction of a single-span railway bridge, forced vibration testing and simulation, Structure and Infrastructure Engineering 21 (1) (2025) 39–48.
21. A. Andersson, J. Östlund, M. Ülker-Kaustell, J.-M. Battini, R. Karoumi, Full-scale dynamic testing of a railway bridge using a hydraulic exciter, in: Experimental Vibration Analysis for Civil Structures: Testing, Sensing, Monitoring, and Control 7, Springer, 2018, pp. 354–363.
22. R. L. Kuhlemeyer, J. Lysmer, Finite element method accuracy for wave propagation problems, Journal of the Soil Mechanics and Foundations Division 99 (5) (1973) 421–427.